Molecular Switches

How to cite: *Angew. Chem. Int. Ed.* **2021**, *60*, 313–320
International Edition: doi.org/10.1002/anie.202009235
German Edition: doi.org/10.1002/ange.202009235

Light-Controlled Regioselective Synthesis of Fullerene Bis-Adducts

Luka Đorđević, Lorenzo Casimiro, Nicola Demitri, Massimo Baroncini, Serena Silvi, Francesca Arcudi, Alberto Credi,* and Maurizio Prato**

Dedicated to Prof. Fred Wudl on the occasion of his 80th birthday

Abstract: *Multi-functionalization and isomer-purity of fullerenes are crucial tasks for the development of their chemistry in various fields. In both current main approaches—tether-directed covalent functionalization and supramolecular masks—the control of regioselectivity requires multi-step synthetic procedures to prepare the desired tether or mask. Herein, we describe light-responsive tethers, containing an azobenzene photoswitch and two malonate groups, in the double cyclopropanation of [60]fullerene. The formation of the bis-adducts and their spectroscopic and photochemical properties, as well as the effect of azobenzene photoswitching on the regiochemistry of the bis-addition, have been studied. The behavior of the tethers depends on the geometry of the connection between the photoactive core and the malonate moieties. One tether lead to a strikingly different adduct distribution for the E and Z isomers, indicating that the covalent bis-functionalization of C_{60} can be controlled by light.*

Introduction

Fullerenes and their derivatives, ever since their discovery,[1] have gained interest in a variety of fields ranging from (bio)medical chemistry[2] to material science,[3] with notable advances in thin-film solar cells, such as organic photovoltaic (OPVs) and perovskite solar cells (PSCs).[4] These compounds exhibit a robust electron-deficient character and great semiconducting properties, which have prompted their widespread use as electron acceptors in bulk heterojunction OPVs. Furthermore, fullerenes have emerged as candidates for use in PSC, due to their electron-transport properties and well-matched energy levels with perovskites.[5]

Among fullerene derivatives, the bis-functionalized ones have been the best performing ones in OPVs and PSCs. For example, the pure α-bis-phenyl-C_{62}-butyric acid methyl ester isomer (or α-bis-$PC_{60}BM$) has shown better performance and stability when compared to the more popular mono-functionalized $PC_{60}BM$.[6] Isomerically pure fullerene bis-adducts have also beneficial effects on the performance of OPV devices, when compared to mixtures of isomers, due to their molecular packing.[7] Therefore, devising synthetic approaches towards isomer-pure multi-functionalized fullerenes is desirable for boosting their application, including (but not limited to) the thin-film solar cells area.

Given the spherical nature of [60]fullerene, with its 30 [6,6] double bonds, a precise control of the functionalization reactions that lead to multiple adducts is highly challenging. Specifically, the double addition of symmetric and identical moieties to [60]fullerene can afford 8 regioisomers, which can be described based on the position of the second addend in reference to the first one (Figure 1 a): the former can lie in the same hemisphere (*cis*), at the equator (*e*), or in the opposite hemisphere (*trans*).[8] To control the synthesis of the bis-

[*] L. Đorđević, F. Arcudi, M. Prato
Department of Chemical and Pharmaceutical Sciences & INSTM, UdR Trieste, University of Trieste
via Licio Giorgieri 1, 34127 Trieste (Italy)
E-mail: dordevic.luka@gmail.com
prato@units.it

L. Đorđević, F. Arcudi
Present address: Department of Chemistry, Northwestern University
2145 Sheridan Road, Evanston, IL 60208 (USA)

L. Đorđević
Present address: Simpson Querrey Institute, Northwestern University
303 E. Superior, Chicago, IL 60611 (USA)

L. Casimiro, M. Baroncini, S. Silvi, A. Credi
CLAN—Center for Light Activated Nanostructures, Università di Bologna and Consiglio Nazionale delle Ricerche
via Gobetti 101, 40129 Bologna (Italy)
E-mail: alberto.credi@unibo.it

L. Casimiro, S. Silvi
Dipartimento di Chimica "G. Ciamician", Università di Bologna
via Selmi 2, 40127 Bologna (Italy)

L. Casimiro
Present address: Supramolecular and Macromolecular Photochemistry and Photophysics, ENS Paris-Saclay, CNRS, Université Paris-Saclay
61 Avenue du Président Wilson, 94235 Cachan (France)

N. Demitri
Elettra—Sincrotrone Trieste
S.S. 14 Km 163.5 in Area Science Park, 34149 Basovizza (Italy)

M. Baroncini
Dipartimento di Scienze e Tecnologie Agro-alimentari, Università di Bologna
viale Fanin 44, 40127 Bologna (Italy)

A. Credi
Dipartimento di Chimica Industriale "Toso Montanari", Università di Bologna
viale del Risorgimento 4, 40136 Bologna (Italy)

M. Prato
Center for Cooperative Research in Biomaterials (CIC biomaGUNE), Basque Research and Technology Alliance (BRTA)
Paseo de Miramón 182, 20014 Donostia San Sebastián (Spain)

M. Prato
Basque Foundation for Science
Ikerbasque, Bilbao 48013 (Spain)

Supporting information and the ORCID identification number(s) for the author(s) of this article can be found under: https://doi.org/10.1002/anie.202009235.

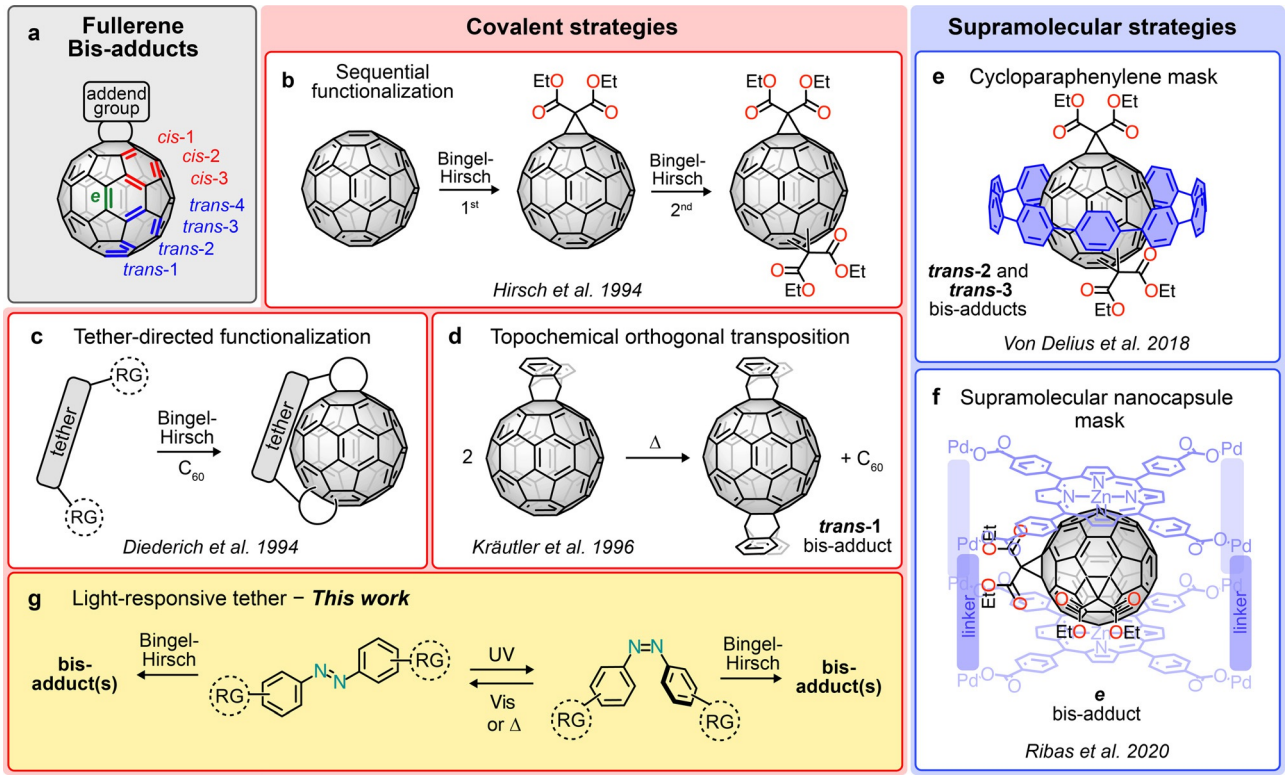

Figure 1. Current synthetic strategies towards regioselective bis-functionalization of fullerene C_{60} (a) can be divided in two categories: covalent (b–d) and supramolecular (e–f). The approach described in this work (g) belongs to the first category and takes advantage of tether-like compounds. RG = reactive group.

adducts and avoid tedious and time-consuming chromatographic separations, which are necessary for sequential stoichiometric additions such as Bingel-Hirsch cyclopropanation reactions (Figure 1 b),[8] several covalent and supramolecular approaches have been developed (Figure 1 c–f).

The first rational approach towards regioselective synthesis was based on tether-directed remote functionalization.[9] C_{60} was first functionalized with a carboxylic acid anchor group through the Bingel reaction, followed by condensation with a tether carrying a reactive group—a 1,3-butadiene moiety capable of a Diels–Alder addition—leading to the *equatorial* bis-adduct in 23 % yield. This approach was then extended to the tether-directed double addition by exploiting tethered bis-malonates which, after reaction with C_{60}, afforded bis-adducts in a shorter synthetic route (Figure 1 c).[10] Since then, numerous tether-controlled methods for preparing bis-adducts by double Bingel, 1,3-dipolar or diazo cycloadditions have been described.[11] Also notable is the topochemically controlled Diels–Alder synthesis of *trans*-1 bis-adducts (Figure 1 d), which enabled further functionalization of the available axial positions.[12]

Another elegant approach towards the regiochemical control of multiple additions makes use of supramolecular masks, which could be removed after the reaction (Figure 1ef). This approach consists in confining, before the cycloaddition reactions, C_{60} in supramolecular receptors, such as coordination cages,[13] metal-organic frameworks,[14] covalent organic cages,[15] rotaxanes[16] or cycloparaphenylene (CPP) hosts.[17] In particular, an inclusion complex of diethyl ester $C_{61}(CO_2Et)_2$ and [10]CPP, when subjected to a Bingel cyclopropanation, yielded *trans*-3 and *trans*-2 $C_{62}(CO_2Et)_4$ in 24 % and 20 % yields, respectively (Figure 1 e). Recently, a metallosupramolecular cuboid box-shaped host was used to complex C_{60}, leaving four openings that direct the cyclopropanation reactions in the equatorial position in 97 % yield (Figure 1 f).[13c] However, all the regioselective methods reported to date, despite their elegance, lack flexibility and require significant efforts, because a specific tether or supramolecular mask has to be designed and prepared to target one (or more) regioisomers.

An appealing strategy towards more versatile routes to regioselective fullerene bis-functionalization is to combine tether-directed double addition methods with molecular switching by an external trigger. Molecular switches—species that can be reversibly interconverted between different forms in response to chemical or physical stimuli—offer a wealth of possibilities in terms of structure, properties, and nature of the control input.[18] Light is a very convenient tool to operate molecular switches, particularly in multi-component systems, because it is a non-invasive signal that can be carefully modulated in time, space and energy.[18,19] There have been previous reports of photoswitches and fullerenes[31] that have focused on the photoisomerization of fullerene dimers[20] and using tweezers for the supramolecular encapsulation of C_{60}.[21]

Here we investigate the use of photoswitchable tethers for the regioselective bis-addition to C_{60} fullerene (Figure 1 g).

As the light-responsive moiety we chose azobenzene because of its facile functionalization and well known photoisomerization process.[22] Generally, the *E* isomer is thermodynamically stable and it is converted to the *Z* isomer by UV light irradiation; the *E* form can be regenerated thermally or by exposure to visible light. As the *E*-*Z* transformation is accompanied by a large geometrical rearrangement and a change in the length of the azobenzene moiety, we envisaged that if the latter is endowed with two terminal units capable of attacking the C_{60} double bonds, then the *E* and *Z* isomers could undergo the bis-addition with different regiochemical outcomes. On the other hand, the photochemical properties of the azobenzene unit could be modified upon covalent attachment to the fullerene. To investigate these points, we prepared two molecular tethers consisting of an azobenzene core and two malonate reactive end groups. The two tethers, which differ in the substitution position of the malonate groups on the phenyl rings of the azobenzene, were employed in both the *E* and *Z* configurations for the double cyclopropanation reaction on the C_{60} sphere. We also investigated the structural, spectroscopic and photochemical properties of the tethers and their fullerene bis-adducts.

Results and Discussion

Design, synthesis and spectroscopic characterization of the azobenzene tethers

To gain insight on the role of azobenzene configuration, and thus the effect of photoisomerization, on the formation of the C_{60} bis-adducts, we designed two different tethers in which the malonate units are introduced either in *meta* or in *para* positions on the azobenzene aromatic rings (compounds **4** and **6**, respectively, in Scheme 1). Molecular modelling confirms that such substitution patterns lead to different isomer dependence of the distance between the terminal malonates (Supporting Information, Section 6). Moreover, in the less symmetric *meta* derivative the end-to-end distance can also be affected by the rotation of phenyl rings around the C–N bond.[23]

The synthetic route (Scheme 1) involves the reductive coupling of *m*-nitrobenzyl alcohol, using glucose/NaOH[24] as reducing agent, to give azobenzene **3**. The azobenzene diol was subsequently converted, with ethyl malonyl chloride in presence of 4-dimethylaminopyridine,[25] into bis-malonate **4**, containing *meta*-substituted azobenzene. Bis-malonate **6**, with substituents in the *para*-position of azobenzene, whose structure was confirmed also by X-ray crystallography (Supporting Information, Section 5), could be obtained using the same sequence and reaction conditions starting from *p*-nitrobenzyl alcohol. The spectroscopic and (photo)isomerization properties of these two azobenzene derivatives were then investigated in toluene at room temperature (Table S1).

Compound *E*-**4** shows the typical absorption spectrum of azobenzene derivatives:[22a–f] a weak *n*-π* band centered at 450 nm, with a molar absorption coefficient (ε) of $500\,M^{-1}cm^{-1}$, and a more intense π-π* band in the UV region, with maximum at 322 nm and an ε of $22\,000\,M^{-1}cm^{-1}$ (Figure S15). Irradiation of *E*-**4** at 313 nm or 365 nm produces a strong decrease in the UV absorption and an increase of the *n*-π* band (see Figure 2a), which can be ascribed to an $E \rightarrow Z$ isomerization, until a photostationary state (PSS) is achieved. The composition of the PSS was determined from the corresponding absorption spectra by applying the Fischer method[26] and resulted to be $[Z]/[E] = 92{:}8$ at 365 nm and

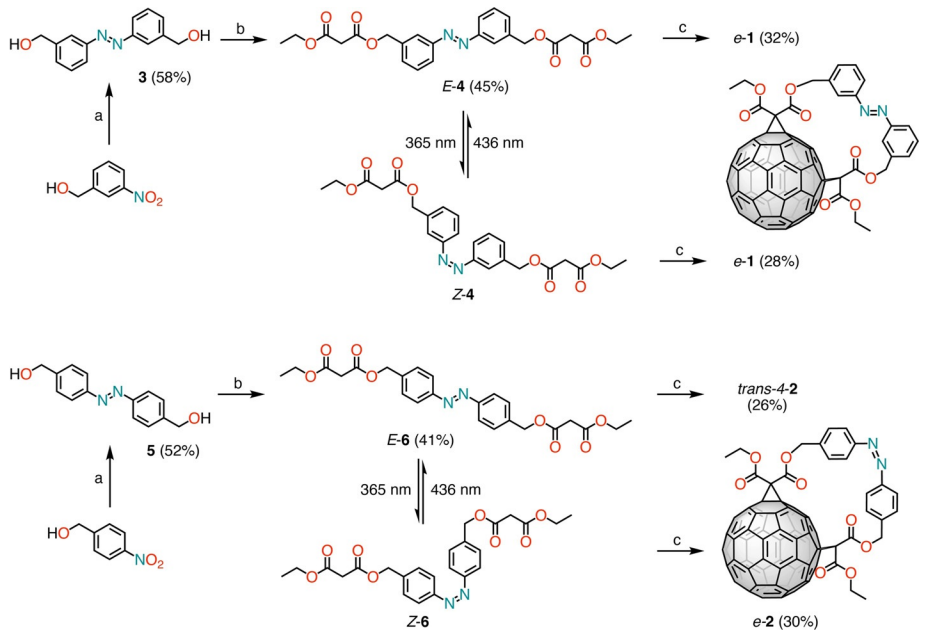

Scheme 1. Synthesis of C_{60} bis-adducts by azobenzene tether-directed remote functionalization. Reagents and conditions: a) D-glucose, NaOH, $EtOH/H_2O$, 50 °C; b) $EtOOCCH_2COCl$, DMAP, an. THF, 0 °C → r.t., 16 h; c) C_{60}, I_2, DBU, toluene, 0 °C, 2 h, dark. DMAP = 4-(dimethylamino)pyridine, THF = tetrahydrofuran, DBU = 1,8-diazabicyclo[5.4.0]undec-7-ene.

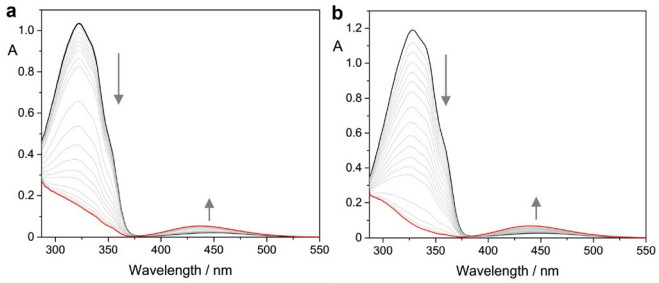

Figure 2. Absorption changes of azobenzene tethers *E*-**4** (a, 47×10^{-6} M) and *E*-**6** (b, 44×10^{-6} M) upon irradiation at 365 nm in toluene at room temperature.

83:17 at 313 nm. With the same method, the absorption spectrum of the *Z* isomer was also calculated. The quantum yield for the $E\rightarrow Z$ isomerization, measured upon irradiation at 365 nm, is 0.18. Upon irradiation in the visible region of a solution previously exhaustively irradiated at 365 nm to reach the PSS, back $Z\rightarrow E$ photoisomerization occurs, until a PSS of 85:15 [*E*]/[*Z*] is afforded. The quantum yield related to this process, measured upon irradiation at 436 nm, resulted to be 0.64. The thermal $Z\rightarrow E$ isomerization was studied by monitoring over several days the absorption changes of a UV-irradiated solution kept in the dark at room temperature. The data could be satisfactorily fitted according to a first order kinetic law, giving a rate constant of $1.4\times10^{-6}\,s^{-1}$ (Figure S16).

Compound *E*-**6** shows an absorption spectrum similar to compound *E*-**4** (Figure S17), but with an overall higher absorption coefficient. The *n*-π* band is centered at 450 nm, with an ε of $660\,M^{-1}cm^{-1}$, and the π-π* band is slightly redshifted with respect to **4**, peaking at 328 nm and with an $\varepsilon = 27000\,M^{-1}cm^{-1}$.

Irradiation of *E*-**6** in the UV induces the $E\rightarrow Z$ isomerization (Figure 2b) until photostationary states, richer in *Z* isomer with respect to **4**, are achieved. The PSS composition and the spectrum of the *Z* form were determined as in the previous case. The percentage of *Z* at the PSS resulted to be 97% at 365 nm and 68% at 313 nm. The quantum yield for the $E\rightarrow Z$ isomerization, measured at 365 nm, is 0.14. As observed for **4**, irradiation in the visible region (436 nm) converts preferentially the *Z* form into the *E* one, however with a quantum yield (0.51) lower than that of compound **4**. The thermal back isomerization, in this case, possesses a rate constant of $2.7\times10^{-6}\,s^{-1}$ (Figure S18).

In summary, the spectroscopic and photochemical behavior of the two tethers is in line with that of azobenzene derivatives, and indicate that the presence of the malonate substituents does not hamper photoswitching. The thermal $Z\rightarrow E$ isomerization process is also present, but it should be emphasized that under the conditions employed to form the bis-adducts (0°C, 2 h reaction time; see Scheme 1) such reaction can be neglected for both **4** and **6** (Figures S19,S20).

Synthesis and spectroscopic characterization of the C_{60} bis-adducts

The reaction of bis-malonate *meta*-substituted azobenzene *E*-**4** with C_{60} by a modified Bingel-Hirsch reaction[27] yielded the *equatorial* bis-adduct **1** in 32% isolated yield (Scheme 1, top). The ^{1}H- and ^{13}C-NMR spectra showed molecular C_1-symmetry (Supporting Information, Figures S5,S6). We were able to grow single crystals of C_{60}-azobenzene derivative *e*-**1**, from hexane vapor diffusion into a chloroform solution, suitable for X-ray crystallography (monoclinic, space group $P2_1/c$). The crystal structure confirmed the C_1 symmetry of the molecule and the *E*-configuration of the azobenzene tether (Figure 3). The transesterification reaction[28] of *e*-**1** yielded tetraethyl ester *e*-$C_{62}(CO_2Et)_4$ (**7**) with C_s symmetry. Furthermore, adduct **1** showed an absorption spectrum (Figure S21) coherent with a bis-functionalized C_{60} in equatorial position and superimposable with the mathematic sum of the absorption spectra of the parent *E*-**4** and the reference tetraethyl ester *e*-$C_{62}(CO_2Et)_4$ (**7**), confirming that the reaction occurred between the *E* isomer and the C_{60}.

For the synthesis of C_{60} bis-adduct using the *Z*-**4** isomer, the $E\rightarrow Z$ photoisomerization of **4** had to be performed on a larger scale and higher concentration (Supporting Information, Figure S32) compared to the spectroscopic studies reported in the previous section. Additionally, it was necessary to perform flash chromatography to isolate the pure *Z* isomer (with 55% isolated yield). The bis-malonate *Z*-**4** was then allowed to react with C_{60} under modified Bingel-Hirsch conditions and, surprisingly, yielded once again the *equatorial*-**1** bis-adduct with the azobenzene in the *E* configuration

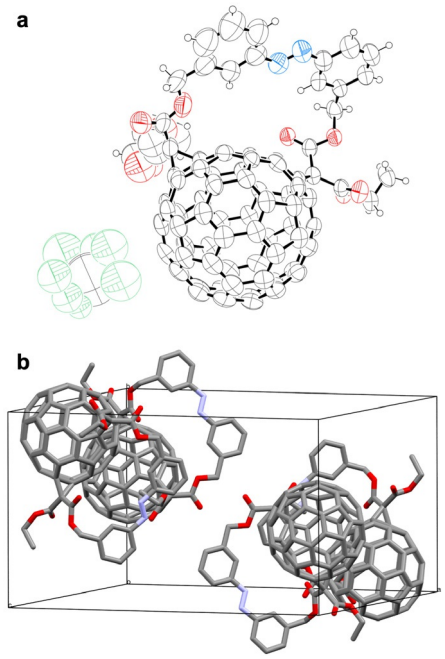

Figure 3. a) Crystal structure (atomic displacement parameters are drawn at the 50% probability level; for CCDC numbers see the Supporting Information) and b) crystal packing (molecules of $CHCl_3$ are omitted for clarity) of the *equatorial* bis-adduct **1**.

(Scheme 1, top). While the reaction was running, monitoring with thin-layer chromatography (TLC) allowed us to detect only *equatorial*-**1** bis-adduct, which was confirmed, after purification, by ^{1}H- and ^{13}C-NMR spectra and UV/Vis spectroscopy.

Indeed, irradiation of bis-adduct *e*-**1** at 365 nm (Figure S22) produced no appreciable variations, even for prolonged exposure times. Thus, the *Z* stereoisomer of *e*-**1** cannot be accumulated by photoirradiation. This observation could be due either to the suppressed photoreactivity of the azo unit (i.e., very low quantum yield) or to a very fast $Z \rightarrow E$ back reaction. It can be hypothesized that the covalent connection of the azobenzene to the fullerene via the malonate tethers may constrain the former in the *E* configuration.[29]

Interestingly, the *para*-substituted azobenzene tether **6** exhibited a completely different behavior (Scheme 1, bottom). The modified Bingel-Hirsch reaction of *E*-**6** with C_{60} afforded a mixture that proved difficult to purify and characterize. However, careful separation of the regioisomers by preparative TLC and their subsequent characterization by UV/Vis spectroscopy, given the characteristic features in the 400–700 nm region used as a fingerprint,[25] allowed us to identify three regioisomers (Figure S34). The main product is the *trans*-4 bis-adduct (91 % relative yield), together with two minor products consisting of the *trans*-2 and *trans*-3 regioisomers (7 % and 2 % relative yields, respectively). Although *trans*-4-**2** shows broad ^{1}H NMR signals (Figure S36), a comparison with the spectra of *E*- and *Z*-**6** (Figure S37) suggests that the azobenzene in the bis-adduct is in the *E* configuration.

We then proceeded with the photoisomerization of *E*-**6** to *Z*-**6**, following the same procedure employed for the *meta*-substituted azobenzene. The bis-malonate *Z*-**6**, obtained with isolated 75 % yield, was allowed to react with C_{60} under modified Bingel-Hirsch conditions.[27] The *equatorial* derivative **2** was obtained as the main product in 30 % isolated yield. The relative positions of the two cyclopropane rings on the C_{60} were discerned by ^{1}H-NMR, ^{13}C-NMR, UV/Vis spectroscopy and X-ray crystallography. The ^{1}H and ^{13}C-NMR spectra confirmed the C_1 symmetry of compound *e*-**2**, especially evident from the 56 signals from the sp^2 fullerene C atoms (Supporting Information, Figure S28). We were also able to grow single crystals of C_{60}-azobenzene derivative *e*-**2**, from hexane vapor diffusion into a chloroform solution, suitable for X-ray crystallography (triclinic, space group $P\bar{1}$). The crystal structure confirmed the *Z* configuration of the azobenzene unit and the C_1 symmetry of the molecule (Figure 4ab). Further confirmations were obtained by UV/Vis spectroscopy, which showed characteristic features of *equatorial* C_{60} bis-adducts in the 400–700 nm region (Figure 4c).[25] Finally, transesterification reaction (K_2CO_3, anhydrous THF/EtOH 1:1 *v*/*v*, r.t.) of compound *e*-**2** yielded the known tetraethyl ester *e*-$C_{62}(CO_2Et)_4$ (**7**) with C_s symmetry.[8,28]

Irradiation of compound *e*-**2** in the visible region at 436 nm produced little changes in the absorption spectrum, which could be ascribed to a $Z \rightarrow E$ isomerization, with an estimated quantum yield of 0.11. In another experiment, we irradiated the sample at 436 nm for a few minutes and then at 365 nm to trigger the $E \rightarrow Z$ transformation (Figure 4d). The

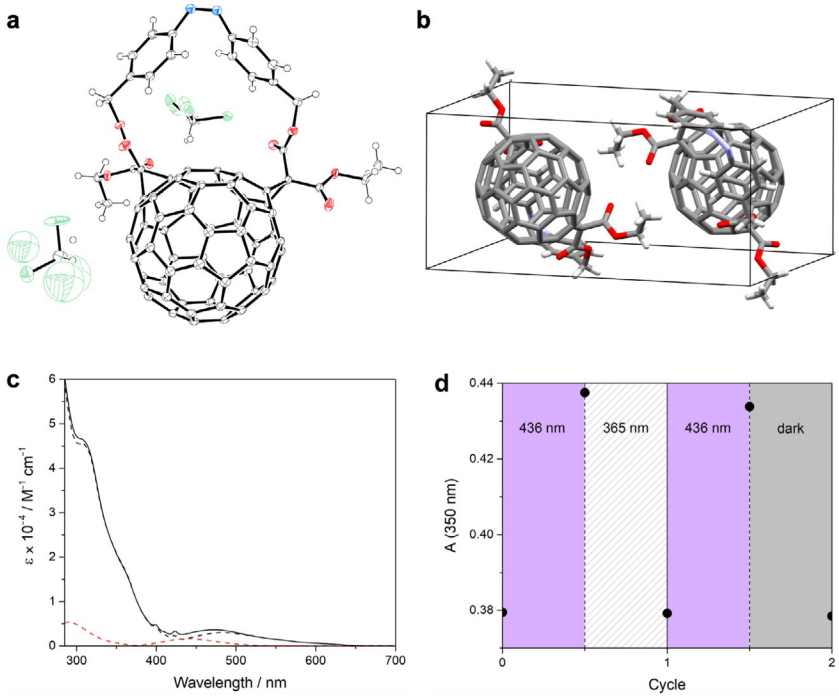

Figure 4. a) Crystal structure (atomic displacement parameters are drawn at the 50 % probability level; for CCDC numbers see the Supporting Information) and b) crystal packing (molecules of $CHCl_3$ are omitted for clarity) of *equatorial* bis-adduct **2**. c) Absorption spectrum of **2** (black full line) in toluene, together with the spectra of *Z*-**6** (red dashed line) and **7** (black dashed line). d) Absorbance changes upon successive irradiations at 436 nm (purple areas) and 365 nm (striped area), and final rest in the dark (grey area).

initial spectrum was regenerated, confirming that the photoreaction is the $Z \rightarrow E$ isomerization. After a successive irradiation at 436 nm, the solution was kept in the dark and its absorbance monitored over time. The photoproduct exhibits a relatively fast thermal back isomerization in the dark to the initial *Z*-form; the transformation is complete within one hour at room temperature (rate constant 1.0×10^{-3} s^{-1}, Figure S24).

All these data suggest that the thermodynamically stable form of the azo moiety in the bis-adduct *e*-**2** is *Z*. Irradiation at 436 nm can produce the *E* isomer, although with a much lower quantum yield than that observed for the same reaction in the free tether **6** (Table S1). Interestingly, the metastable form of *e*-**2** reverts back to the stable configuration with a rate constant three orders of magnitude faster than that of the analogous process in tether **6**.

Structural features of the tethers and regioselectivity of the bis-adducts

Aimed at rationalizing the observed results, we compared the outcomes of the four bis-addition cyclopropanation reactions, and attempted to correlate them with the structure of the tethers. A conformational/configurational analysis performed by DFT calculations enabled us to determine the length of the switchable unit of tethers **4** and **6** in their *E* and *Z* forms, taken as the distance between the methylene carbon atoms connecting the azobenzene core with the malonate moieties (d_{core}; Supporting Information, Section 6). Although the conformational freedom of each malonate group can also play a role in the bis-addition, it can be reasoned that the separation between the malonates will be largely determined by the more rigid and switchable azobenzene core.

In brief, the calculations show that for both tethers the *E* configuration is more stable than the *Z* (Tables S3,S4), albeit in **4** the energy difference (3.5 kcal mol^{-1}) is much smaller than that of **6** (9.8 kcal mol^{-1}) and of plain azobenzene (ca. 12 kcal mol^{-1}).[22a] In both cases the $E \rightarrow Z$ isomerization causes a significant decrease of d_{core} (35–40 %); however, in the case of **4** the "off-axis" *meta*-substitution determines, in each configuration, the presence of *syn* and *anti* conformations of the malonates with respect to the azobenzene main axis, in which d_{core} can change by ± 10 % (Table S3 and Figure S39). On the contrary, d_{core} in the *para*-derivative **6** depends exclusively on the azobenzene configuration (Table S4 and Figure S40).

In the case of the *meta*-substituted tether (**4**), we did not observe substantial differences, in terms of regioisomer distribution and product yields, between the *E* and *Z* forms. The d_{core} parameter computed for the stable conformer of *E*-**4** (9.16 Å) is very similar to the analogous distance measured from the X-ray structure of *e*-**1** (8.87 Å, Figure 3 a). This observation explains the ability of **4** in its *E* form to doubly functionalize C_{60} with an equatorial pattern. On the other hand, the stable conformer of *Z*-**4** has a much shorter extension ($d_{core} = 5.45$ Å), most likely incompatible with an equatorial bis-addition. This finding, together with the fact that the reaction between *Z*-**4** and C_{60} forms a bis-adduct with the azobenzene unit in the *E* configuration, indicates that the bis-addition can only occur with the tether in its *E* form. Furthermore, our data show that the thermal isomerization of free *Z*-**4** is too slow to account for the formation of a significant amount of *E*-**4** on the cyclopropanation time scale. Hence, we propose that a mono-adduct between *Z*-**4** and C_{60} is formed first, in which the thermal $Z \rightarrow E$ isomerization is strongly accelerated, possibly because of electronic interactions between the fullerene sphere and the dangling azobenzene and/or malonate units. As the rate of the first addition is likely unaffected by the isomeric form of the azobenzene unit, *e*-**1** is obtained in similar yields irrespective of the initial configuration of the tether. Finally, the impossibility to accumulate the *Z* form of *e*-**1** by light irradiation is consistent with such a scenario.

The results are markedly different—and more interesting—in the case of the *para*-substituted tether **6**, with the *E*- or *Z*-**6** bis-malonate tethers exhibiting different regioselectivities (Figure 5, Figures S34–S37). Subjecting bis-malonate *E*-**6** to the modified Bingel-Hirsch reaction gave bis-adducts *trans*-4, *trans*-3 and *trans*-2 in 91 %, 2 % and 7 % relative yields, respectively. Conversely, the *Z*-isomer of **6** afforded bis-adducts *e*, *cis*-3, *trans*-4, *trans*-3 and *trans*-2 in 81 %, 10 %, 6 %, 1 % and 2 % relative yields,[30] respectively. DFT Calculations show that in *E*-**6** d_{core} can be as large as 12.5 Å, whereas it is 7.96 Å in *Z*-**6**. The experimental distance found in the crystal structure of *e*-**2** (9.02 Å, Figure 4 a) correlates reasonably well with the latter value, whereas it is considerably shorter than the former one. This comparison provides a rationale for both the propensity of *Z*-**6** to equatorial bis-addition and the stabilization of the *Z*-azobenzene unit with respect to the *E*-form in the adduct *e*-**2**. On the other hand, the larger d_{core} in *E*-**6** could favor *trans* bis-addition patterns with respect to the equatorial one, thus qualitatively explaining the observed regioselectivity and the *E* configuration of the azobenzene unit in *trans*-4-**2**.

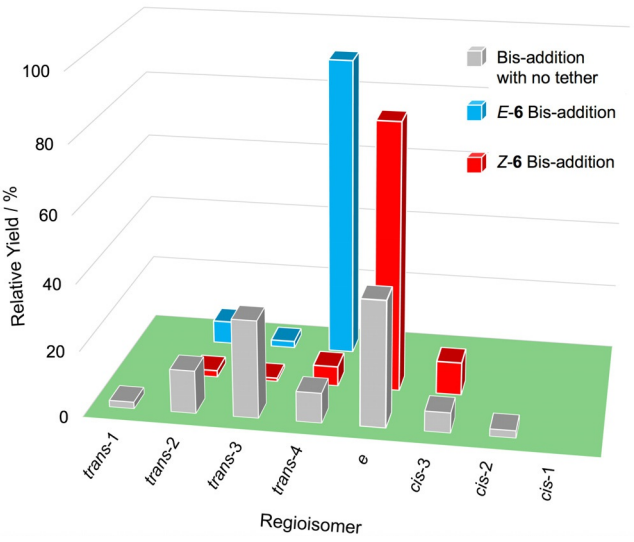

Figure 5. Relative reaction yields of the regioisomeric Bingel-Hirsch bis-adducts of *E*-**6** (blue bars) and *Z*-**6** (red bars) azobenzene tethers, and published data[8] in the absence of tethers (grey bars).

Conclusion

Two photoswitchable azobenzene derivatives, each bearing two malonate reactive groups in *meta*- or *para*- positions to the azo moiety, were used as tethers for the preparation of [60]fullerene bis-adducts. Molecular modelling shows that, despite the structural similarity, the two compounds exhibit different behavior with regard to photoinduced shape modifications. In the case of the *meta*-substituted azobenzene tether, the bis-addition regioselectivity does not change when using either the *E* or the *Z* isomers. The main product, in both cases, is the *equatorial* bis-adduct, in which the azobenzene unit is in the *E* configuration and loses its photoswitching capacity because of the steric strain caused by the covalent linkage to C_{60}.

The *para*-substituted tether gives more interesting results, as the regioselectivity of the double cyclopropanation reaction is markedly different for the *E* and Z isomers. The *E*-tether, characterized by a longer length of the azobenzene core, forms preferentially *trans*-bis-adducts, whereas for the *Z*-tether the equatorial bis-addition prevails. Furthermore, in the latter adduct the azobenzene unit exists in the *Z* form, which becomes the thermodynamically stable one as shown by single crystal X-ray diffraction and spectroscopic and photochemical experiments.

These findings are significant because they show that the light-responsive properties of a molecular moiety can be modulated by covalent attachment to the C_{60} sphere, in a way that depends on the bis-functionalization pattern, thus creating new opportunities in the field of photochromism.

Moreover, this work provides the basis for alternative routes to fullerene functionalization, in which light can be employed as a tool to direct the reaction outcome by taking advantage of molecular photoswitching. Such a general approach, characterized by simplicity and versatility, could lead to the controlled production of fullerene isomers of interest as active materials in organic and perovskite solar cells. It is tempting to think that this strategy, based on using light to control the regiochemistry of a non-photochemical reaction, could be applied to other fullerenes and multi-adducts, as well as other substrates and (photo)switches.

Acknowledgements

This work was supported by the University of Trieste and the Maria de Maeztu Units of Excellence Program from the Spanish State Research Agency (Grant No. MDM-2017-0720). Additional financial support from the Ministero dell'Istruzione, Università e Ricerca (PRIN grants 2017PBXPN4, 20173L7W8K and 201732PY3X, and FARE grant R16S9XXKX3), the University of Bologna, and the National Research Council of Italy is gratefully acknowledged. We thank Prof. Tatiana Da Ros and Dr. Giulio Ragazzon (University of Trieste), and Profs. Ettore Fois and Gloria Tabacchi (University of Insubria) for their help with the HPLC and DFT calculations, respectively.

Conflict of interest

The authors declare no conflict of interest.

Keywords: azobenzene · fullerenes · molecular switches · photoswitches · regioselectivity

[1] a) H. W. Kroto, J. R. Heath, S. C. O'Brien, R. F. Curl, R. E. Smalley, *Nature* **1985**, *318*, 162 – 163; b) N. Martín, *Chem* **2019**, *5*, 733 – 738.

[2] a) S. Bosi, T. Da Ros, G. Spalluto, M. Prato, *Eur. J. Med. Chem.* **2003**, *38*, 913 – 923; b) I. Nierengarten, J. F. Nierengarten, *Chem. Asian J.* **2014**, *9*, 1436 – 1444; c) E. Castro, A. Hernandez Garcia, G. Zavala, L. Echegoyen, *J. Mater. Chem. B* **2017**, *5*, 6523 – 6535; d) J. Ramos-Soriano, J. J. Reina, B. M. Illescas, N. de la Cruz, L. Rodriguez-Perez, F. Lasala, J. Rojo, R. Delgado, N. Martin, *J. Am. Chem. Soc.* **2019**, *141*, 15403 – 15412.

[3] a) A. Montellano López, A. Mateo-Alonso, M. Prato, *J. Mater. Chem.* **2011**, *21*, 1305 – 1318; b) L. Đorđević, T. Marangoni, F. De Leo, I. Papagiannouli, P. Aloukos, S. Couris, E. Pavoni, F. Monti, N. Armaroli, M. Prato, D. Bonifazi, *Phys. Chem. Chem. Phys.* **2016**, *18*, 11858 – 11868.

[4] a) W. Yan, S. M. Seifermann, P. Pierrat, S. Bräse, *Org. Biomol. Chem.* **2015**, *13*, 25 – 54; b) T. Umeyama, H. Imahori, *Dalton Trans.* **2017**, *46*, 15615 – 15627; c) T. Gatti, E. Menna, M. Meneghetti, M. Maggini, A. Petrozza, F. Lamberti, *Nano Energy* **2017**, *41*, 84 – 100; d) A. Zieleniewska, F. Lodermeyer, A. Roth, D. M. Guldi, *Chem. Soc. Rev.* **2018**, *47*, 702 – 714; e) E. Castro, J. Murillo, O. Fernandez-Delgado, L. Echegoyen, *J. Mater. Chem. C* **2018**, *6*, 2635 – 2651; f) S. Collavini, J. L. Delgado, *Sustainable Energy Fuels* **2018**, *2*, 2480 – 2493; g) M. Izquierdo, B. Platzer, A. J. Stasyuk, O. A. Stasyuk, A. A. Voityuk, S. Cuesta, M. Sola, D. M. Guldi, N. Martín, *Angew. Chem. Int. Ed.* **2019**, *58*, 6932 – 6937; *Angew. Chem.* **2019**, *131*, 7006 – 7011.

[5] a) J. Y. Jeng, Y. F. Chiang, M. H. Lee, S. R. Peng, T. F. Guo, P. Chen, T. C. Wen, *Adv. Mater.* **2013**, *25*, 3727 – 3732; b) D. Luo, W. Yang, Z. Wang, A. Sadhanala, Q. Hu, R. Su, R. Shivanna, G. F. Trindade, J. F. Watts, Z. Xu, T. Liu, K. Chen, F. Ye, P. Wu, L. Zhao, J. Wu, Y. Tu, Y. Zhang, X. Yang, W. Zhang, R. H. Friend, Q. Gong, H. J. Snaith, R. Zhu, *Science* **2018**, *360*, 1442 – 1446; c) M. Hadadian, J.-H. Smått, J.-P. Correa-Baena, *Energy Environ. Sci.* **2020**, *13*, 1377 – 1407; d) X. Zheng, Y. Hou, C. Bao, J. Yin, F. Yuan, Z. Huang, K. Song, J. Liu, J. Troughton, N. Gasparini, C. Zhou, Y. Lin, D.-J. Xue, B. Chen, A. K. Johnston, N. Wei, M. N. Hedhili, M. Wei, A. Y. Alsalloum, P. Maity, B. Turedi, C. Yang, D. Baran, T. D. Anthopoulos, Y. Han, Z.-H. Lu, O. F. Mohammed, F. Gao, E. H. Sargent, O. M. Bakr, *Nat. Energy* **2020**, *5*, 131 – 140.

[6] F. Zhang, W. Shi, J. Luo, N. Pellet, C. Yi, X. Li, X. Zhao, T. J. S. Dennis, X. Li, S. Wang, Y. Xiao, S. M. Zakeeruddin, D. Bi, M. Grätzel, *Adv. Mater.* **2017**, *29*, 1606806.

[7] T. Umeyama, H. Imahori, *Acc. Chem. Res.* **2019**, *52*, 2046 – 2055.

[8] A. Hirsch, I. Lamparth, H. R. Karfunkel, *Angew. Chem. Int. Ed. Engl.* **1994**, *33*, 437 – 438; *Angew. Chem.* **1994**, *106*, 453 – 455.

[9] L. Isaacs, R. F. Haldimann, F. Diederich, *Angew. Chem. Int. Ed. Engl.* **1994**, *33*, 2339 – 2342; *Angew. Chem.* **1994**, *106*, 2434 – 2437.

[10] J.-F. Nierengarten, V. Gramlich, F. Cardullo, F. Diederich, *Angew. Chem. Int. Ed. Engl.* **1996**, *35*, 2101 – 2103; *Angew. Chem.* **1996**, *108*, 2242 – 2244.

[11] a) J. F. Nierengarten, T. Habicher, R. Kessinger, F. Cardullo, F. Diederich, V. Grämlich, J. P. Gisselbrecht, C. Boudon, M. Gross, *Helv. Chim. Acta* **1997**, *80*, 2238 – 2276; b) F. Diederich, R. Kessinger, *Acc. Chem. Res.* **1999**, *32*, 537 – 545; c) C. Thilgen, F. Diederich, *C. R. Chim.* **2006**, *9*, 868 – 880; d) V. Garg, G. Kodis, M. Chachisvilis, M. Hambourger, A. L. Moore, T. A. Moore, D. Gust, *J. Am. Chem. Soc.* **2011**, *133*, 2944 – 2954; e) G. Bottari, O.

Trukhina, A. Kahnt, M. Frunzi, Y. Murata, A. Rodríguez-Fortea, J. M. Poblet, D. M. Guldi, T. Torres, *Angew. Chem. Int. Ed.* **2016**, *55*, 11020 – 11025; *Angew. Chem.* **2016**, *128*, 11186 – 11191; f) M. R. Cerón, L. Echegoyen, *J. Phys. Org. Chem.* **2016**, *29*, 613 – 619.

[12] a) B. Kräutler, T. Müller, J. Maynollo, K. Gruber, C. Kratky, P. Ochsenbein, D. Schwarzenbach, H.-B. Bürgi, *Angew. Chem. Int. Ed. Engl.* **1996**, *35*, 1204 – 1206; *Angew. Chem.* **1996**, *108*, 1294 – 1296; b) R. Schwenninger, T. Müller, B. Kräutler, *J. Am. Chem. Soc.* **1997**, *119*, 9317 – 9318.

[13] a) W. Brenner, T. K. Ronson, J. R. Nitschke, *J. Am. Chem. Soc.* **2017**, *139*, 75 – 78; b) B. Chen, J. J. Holstein, S. Horiuchi, W. G. Hiller, G. H. Clever, *J. Am. Chem. Soc.* **2019**, *141*, 8907 – 8913; c) C. Fuertes-Espinosa, C. García-Simón, M. Pujals, M. Garcia-Borràs, L. Gómez, T. Parella, J. Juanhuix, I. Imaz, D. Maspoch, M. Costas, X. Ribas, *Chem* **2020**, *6*, 169 – 186.

[14] N. Huang, K. Wang, H. Drake, P. Cai, J. Pang, J. Li, S. Che, L. Huang, Q. Wang, H. C. Zhou, *J. Am. Chem. Soc.* **2018**, *140*, 6383 – 6390.

[15] V. Leonhardt, S. Fimmel, A.-M. Krause, F. Beuerle, *Chem. Sci.* **2020**, *11*, 8409 – 8415.

[16] M. Carini, T. Da Ros, M. Prato, A. Mateo-Alonso, *ChemPhysChem* **2016**, *17*, 1823 – 1828.

[17] Y. Xu, R. Kaur, B. Wang, M. B. Minameyer, S. Gsänger, B. Meyer, T. Drewello, D. M. Guldi, M. Von Delius, *J. Am. Chem. Soc.* **2018**, *140*, 13413 – 13420.

[18] a) *Molecular Switches*, 2nd ed., Wiley-VCH, Weinheim, **2011**; b) J. D. Harris, M. J. Moran, I. Aprahamian, *Proc. Natl. Acad. Sci. USA* **2018**, *115*, 9414 – 9422.

[19] a) M. Baroncini, M. Canton, L. Casimiro, S. Corra, J. Groppi, M. La Rosa, S. Silvi, A. Credi, *Eur. J. Inorg. Chem.* **2018**, 4589 – 4603; b) J. Boelke, S. Hecht, *Adv. Opt. Mater.* **2019**, *7*, 1900404; c) G. Naren, C. W. Hsu, S. Li, M. Morimoto, S. Tang, J. Hernando, G. Guirado, M. Irie, F. M. Raymo, H. Sunden, J. Andreasson, *Nat. Commun.* **2019**, *10*, 3996; d) Z. L. Pianowski, *Chem. Eur. J.* **2019**, *25*, 5128 – 5144; e) D. Villaron, S. J. Wezenberg, *Angew. Chem. Int. Ed.* **2020**, *59*, 13192 – 13202; *Angew. Chem.* **2020**, *132*, 13292 – 13302.

[20] J. Zhang, K. Porfyrakis, J. J. L. Morton, M. R. Sambrook, J. Harmer, L. Xiao, A. Ardavan, G. A. D. Briggs, *J. Phys. Chem. C* **2008**, *112*, 2802 – 2804.

[21] a) M. Samanta, A. Rananaware, D. N. Nadimetla, S. A. Rahaman, M. Saha, R. W. Jadhav, S. V. Bhosale, S. Bandyopadhyay, *Sci. Rep.* **2019**, *9*, 9670; b) H. Barbero, S. Ferrero, L. Alvarez-Miguel, P. Gomez-Iglesias, D. Miguel, C. M. Alvarez, *Chem. Commun.* **2016**, *52*, 12964 – 12967.

[22] a) E. Merino, M. Ribagorda, *Beilstein J. Org. Chem.* **2012**, *8*, 1071 – 1090; b) H. M. D. Bandara, S. C. Burdette, *Chem. Soc. Rev.* **2012**, *41*, 1809 – 1825; c) M. Baroncini, G. Ragazzon, S. Silvi, M. Venturi, A. Credi, *Pure Appl. Chem.* **2015**, *87*, 537 – 545; d) L. Dong, Y. Feng, L. Wang, W. Feng, *Chem. Soc. Rev.* **2018**, *47*, 7339 – 7368; e) V. Y. Chang, C. Fedele, A. Priimagi, A. Shishido, C. J. Barrett, *Adv. Opt. Mater.* **2019**, *7*, 1900091; f) M. Baroncini, J. Groppi, S. Corra, S. Silvi, A. Credi, *Adv. Opt. Mater.* **2019**, *7*, 1900392; g) M. Lahikainen, H. Zeng, A. Priimagi, *Nat. Commun.* **2018**, *9*, 4148; h) C. Nacci, M. Baroncini, A. Credi, L. Grill, *Angew. Chem. Int. Ed.* **2018**, *57*, 15034 – 15039; *Angew. Chem.* **2018**, *130*, 15254 – 15259; i) X. Liu, J. Zhang, M. Fadeev, Z. Li, V. Wulf, H. Tian, I. Willner, *Chem. Sci.* **2019**, *10*, 1008 – 1016; j) A. Galanti, J. Santoro, R. Mannancherry, Q. Duez, V. Diez-Cabanes, M. Valasek, J. De Winter, J. Cornil, P. Gerbaux, M. Mayor, P. Samorì, *J. Am. Chem. Soc.* **2019**, *141*, 9273 – 9283; k) D. Mutruc, A. Goulet-Hanssens, S. Fairman, S. Wahl, A. Zimathies, C. Knie, S. Hecht, *Angew. Chem. Int. Ed.* **2019**, *58*, 12862 – 12867; *Angew. Chem.* **2019**, *131*, 12994 – 12999; l) L. Pesce, C. Perego, A. B. Grommet, R. Klajn, G. M. Pavan, *J. Am. Chem. Soc.* **2020**, *142*, 9792 – 9802.

[23] R. L. Klug, R. Burcl, *J. Phys. Chem. A* **2010**, *114*, 6401 – 6407.

[24] S. Ameerunisha, P. S. Zacharias, *J. Chem. Soc. Perkin Trans. 2* **1995**, 1679 – 1682.

[25] F. Djojo, A. Herzog, I. Lamparth, F. Hampel, A. Hirsch, *Chem. Eur. J.* **1996**, *2*, 1537 – 1547.

[26] E. Fischer, *J. Phys. Chem.* **1967**, *71*, 3704 – 3706.

[27] S. Sergeyev, M. Schar, P. Seiler, O. Lukoyanova, L. Echegoyen, F. Diederich, *Chem. Eur. J.* **2005**, *11*, 2284 – 2294.

[28] See Ref [11a].

[29] It cannot be excluded, however, that the behaviour of this particular compound is determined by electronic interactions between the two molecular units.

[30] It is probable that *trans*-2 and *trans*-3 bis-adducts are present in the mixture due to the $Z \rightarrow E$ back isomerization that occurred before the C_{60} functionalization reaction (during chromatographic separation and rotary evaporation).

[31] a) J. Ortíz-Palacios, G. Zaragoza-Galán, E. Aguilar-Ortíz, E. Rodríguez-Alba, E. Rivera, *RSC Adv.* **2017**, *7*, 16751 – 16762; b) P. Lorenz, A. Hirsch, *Chem. Eur. J.* **2020**, *26*, 5220 – 5230; c) D. I. Galimov, A. R. Tuktarov, D. S. Sabirov, A. A. Khuzin, U. M. Dzhemilev, *J. Photochem. Photobiol. A Chem.* **2019**, *375*, 64 – 70.

Manuscript received: July 4, 2020
Accepted manuscript online: July 28, 2020
Version of record online: September 17, 2020

